Innovative Device for Measuring Forces Specific to Various Manufacturing Processes

MIHAIELA ILIESCU[1], GABRIELA TONȚ[2]
[1]Manufacturing Department, [2]Electrical Engineering
[1]"POLITEHNICA" University of Bucharest, [2]University of Oradea
[1]Splaiul Independenței no. 313 Street, [2]Magheru Street no. 7
ROMANIA
iomi@clicknet.ro, gtont@rdslink.ro

Abstract: - Forces that occur into various manufacturing processes usually are worth to be known because of their key role in determining geometrical precision of the manufactured parts, in influencing technological system's rigidity and in reducing energy consumption. The innovative device for measuring these forces is characterized by the shape and dimensions of the elastic element that proves good signal decoupling and the possibility to use it in various manufacturing processes types. The device's prototype was obtained and tested so that, its rigidity characteristics and calibration equations to be determined. Experimented while manufacturing, both in machining and metal forming process, and aided by a LabVIEW data acquisition system, the device made possible the exact determination of each force's component as well as of whole process force's modulus.

Key-Words: - elastic element, manufacturing force, calibration equations, rigidity characteristic

1 Introduction

Manufacturing process is the main stage in obtaining any final part. Its optimization, for both cutting or metal forming processes, is possible [1] only if the dependence relations of the involved factors (variables) are known. Usually, these relations are called *process functions*.

Process forces represent a very important type of process functions, because of their important role in determining geometrical precision of the machined part, in influencing technological system's rigidity and in reducing energy consumption.

Some of the variables manufacturing forces depend on can be mentioned as: part material's characteristics, geometric parameters of the tools being used, values of the manufacturing process' parameters, etc.

Analytical models of manufacturing forces are determined even theoretically – by a theoretical study on defining parameters or, theoretically-experimentally – by choosing some regression type models and determining their constant values, based on experimental data.

The specific literature presents various models - mathematical or graphical ones, for both, cutting and metal forming processes. All of them take into account the influence of different factors, with or without interactions, and their variation range values.

Choosing the one that provides values closer to real ones represents a matter that requires thorough study and good working experience

Measuring manufacturing forces is, usually, performed [4], [5] into laboratories – for experimental–theoretical research or, into production – for adaptive command of the technological system.

The most important component of a force measuring system is the *force measuring device*, whose relevant characteristics are [2]: the load, the exit signal, the calibrating curve, the hysteresis, the rigidity – both static and dynamic. For their proper use, all of these systems have to be calibrated.

The elastic element – meaning it's shape, dimensions, material, etc., represent the key element of the device. The transducers (the study refers to resistive ones) bond on it should "signalize" any kind of its deformation.

Usually, the elastic element is submitted to various loading types and the decoupling of its complex deformation's components is possible only if the transducers are placed in an appropriate number, section and direction.

The manufacturing force measuring devices, that do already exist, have various constructive-functional structures but, are special or specialized ones – meaning they can be used only for a single manufacturing process type.

Once obtained, any force measuring device should be experimentally calibrated.

2 Problem Formulation

Based on the above mentioned aspects, it has been considered of interest [6], the following *objective*: to design, to manufacture and to experimentally-theoretically characterize a device for measuring manufacturing processes' forces.

To achieve the mentioned objective, there have been established the *research directions*, such as:

- designing and obtaining the force measuring device;
- defining and determining of some deformation and rigidity characteristics [3], [6];
- calibrating the device;
- measuring process forces by using the device into various manufacturing systems.

The *research methodology*, consisted in some steps, as follows:

- defining the initial conditions;
- establishing the innovative shape of the elastic element – basic component of the force measuring device
- dimensioning calculus;
- prototype manufacturing;
- theoretically-experimentally determining of deformation and rigidity characteristics;
- theoretically-experimentally determining of the calibrating equation;
- determining some functional and exploitation characteristics by using the device into various manufacturing systems.

3 Problem Solution

As the objective is to obtain the innovative device for measuring forces occurring into various manufacturing process, there have been solved all the problems stated above.

3.1 Elastic Element Design

Most of real situations claim measuring forces that occur into manufacturing systems associated to, both cutting processes (turning, drilling, milling, grinding) and, metal forming processes (punching, bending, drawing, extrusion)

As initial conditions, based on applicative situations, there have been considered *the nominal load*, along each of the main axis, to be of 10,000 N and *the torque*, around each of the main axis to be of 500 N·m (OXYZ being the reference system).

One other important condition was that of good signals' decoupling, regardless loading direction / measuring channel.

The innovative shape of the elastic element (that is the most important part of the force measuring device) consists in a two sides wheel – the upper one rotated by 90° with respect to the lower one, each of them having two spokes.

The dimensions of the elastic element were stated to be: 15 mm in highness and 150 mm in diameter (each side of it). Figure 1 and Figure 2 point out the elastic element's design.

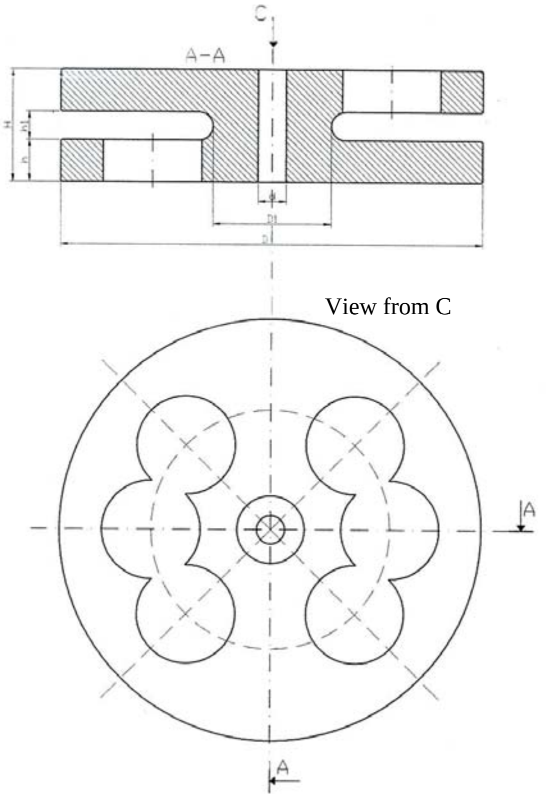

Fig. 1 Elastic element's shape

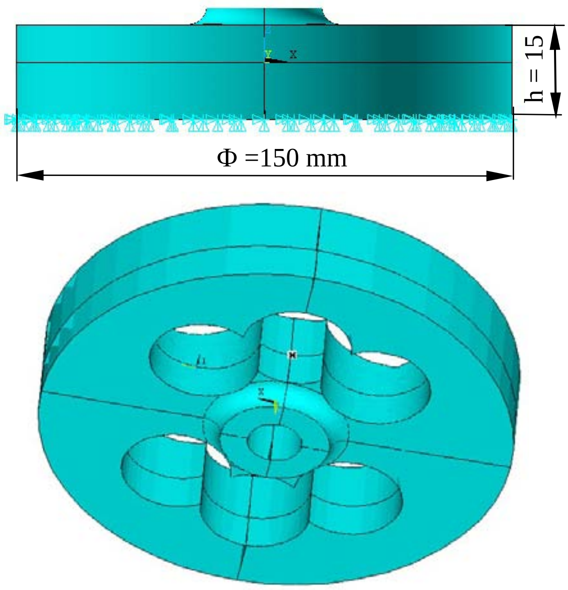

Fig. 2 Elastic element's dimensions

3.2 Prototype Manufacturing

The program used for simulation was ANSYS and with a ten points tetrahedron element there was obtained the parametric model for the study of elastic element behaviour under various loadings.

Because of the constructive and loading symmetry, the simulation can be developed only for one part of the elastic element. The purpose of this modeling is to determine:

- maximum values of equivalent stresses;
- the influence between measured components;
- resistive transducers' position, so as to get maximum sensitivity and lower signal's reciprocal influence.

So, for loading with vertical F_y force (along OY axis of the reference system), the equivalent Von Misses stresses are presented in Figure 3, while the specific deformations, along the indicated line, are pointed out by Figure 4.

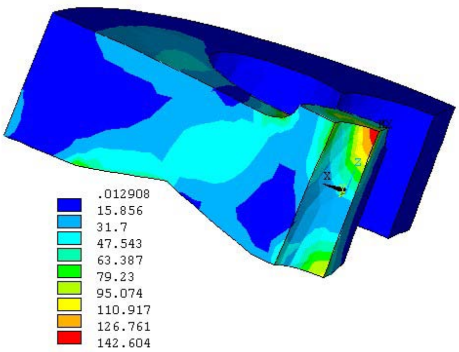

Fig. 3 Equivalent Von Misses stresses for F_y loading

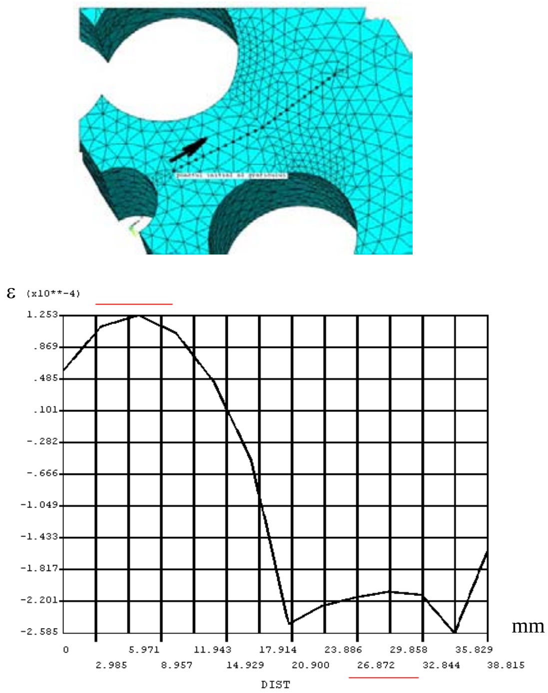

Fig. 4 Specific deformation variation for F_y loading

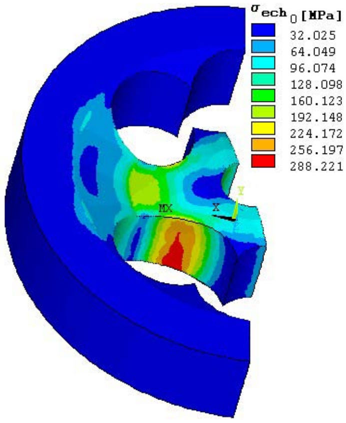

Fig. 5 Equivalent Von Misses stresses for M_y loading

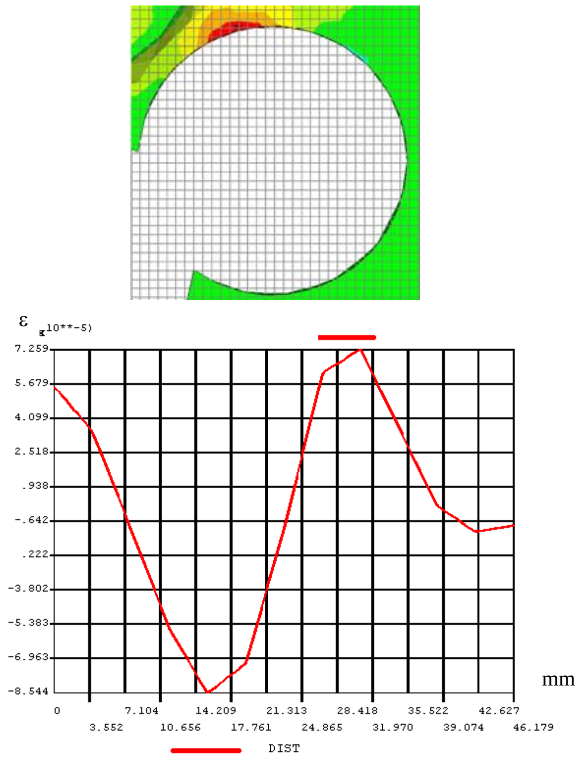

Fig. 6 Specific deformation variation for M_y loading

Similarly, the equivalent Von Misses stresses and the elastic element specific deformation's variation, when loading with M_y torque (around OY axis), are shown by Figure 5 and, respectively, Figure 6.

As result of the whole loading conditions simulation, it was possible to determine optimum position and connection for the resistive transducers used (TER). Examples of transducers' Wheastone bridge connection, for F_y and M_y loading, are presented in Figure 7 and, respectively, Figure 8.

The study of elastic element's rigidity, under dynamic loading, has also been performed, some results being shown by Figure 9.

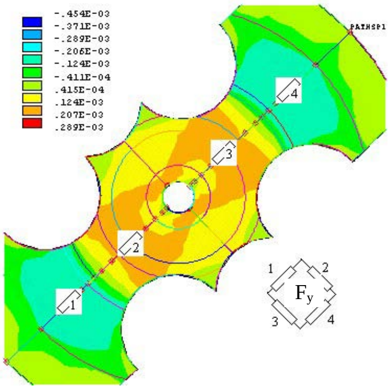

Fig. 7 Transducers position and connection for F_y measuring

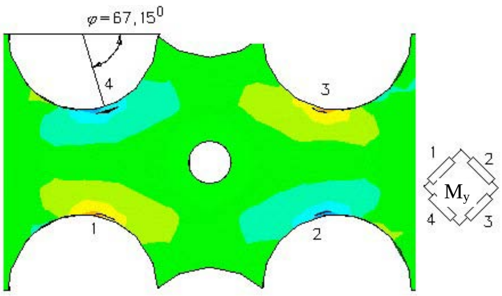

Fig. 8 Transducers position and connection for M_y measuring

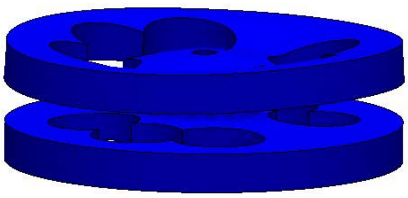

vibration resonance frequency ν_0 = 627,5 Hz

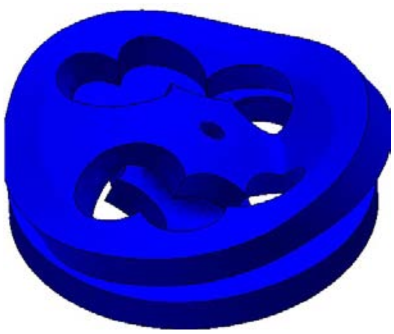

vibration resonance frequency ν_0 = 7182,7 Hz

Fig. 9 Dynamic loading simulation

As result of all the above mentioned aspects, and of more others – screw holes, technological system contact elements - it has been manufactured the force measuring device's prototype. The image of it is presented in Figure 10.

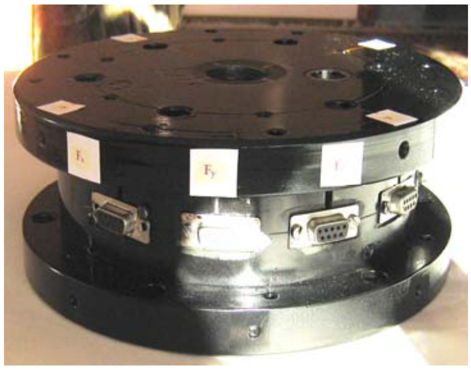

Fig. 10 Force measuring device's prototype

3.3 Deformation and Rigidity Characteristics

Some elements need to be defined, so as to theoretically-experimentally determine deformation and rigidity characteristics. Thus, there are:

- loading force, F; along each of reference system axis, called F_x, F_y and F_z;
- loading forces, F, in XOY, YOZ and XOZ plans, called F_{xy}, F_{yz} and, respectively, F_{zx};
- angles between force direction and reference axis– OX, OY and OZ, φ_x, φ_y, and, respectively, φ_z;
- static resulting deformation, U, along each of the reference system's axis, called X, Y, Z;

The loading force, F, was applied to well defined points (of the device) and, along well defined directions, while the resulting deformation, U, was measured on certain points (of the device).

The deformation characteristic was determined, as graphical dependence:

$$U = U(F) \tag{1}$$

while the strain and rigidity values, C and, respectively, K, were established by relations:

$$C = \frac{U_{max}}{F_{max}}; \quad K = \frac{F_{max}}{U_{max}} \tag{2}$$

Some images, taken while determining of deformation and rigidity characteristics, are presented in Figure 11 – for turning type processes, as well as in Figure 12 – for drilling, milling, punching, bending, etc. manufacturing type processes. There are also presented the corresponding determined static deformation characteristics.

Examples of experimental results, thus obtained, are presented in Table 1 – for turning type processes and, in Table 2 – for drilling, milling, punching, bending, etc. type processes.

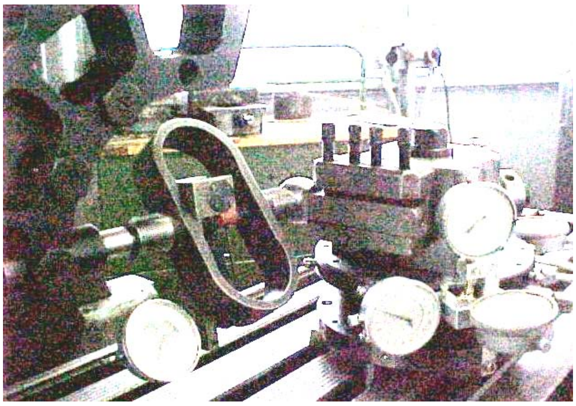

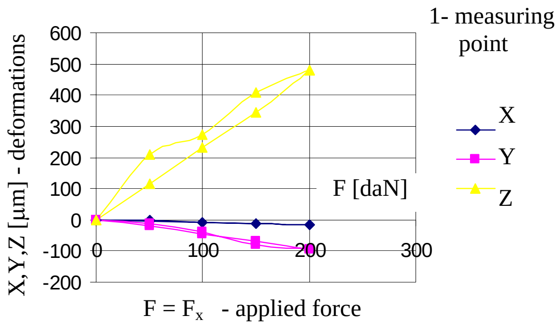

F_x loading force

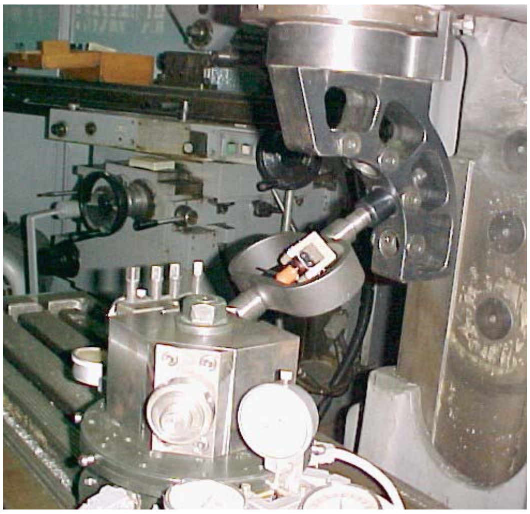

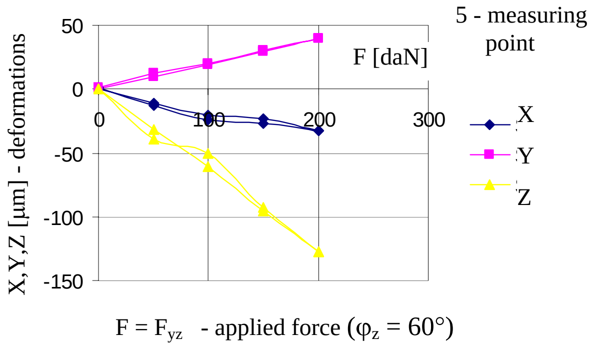

F_{yz} loading force (φ_z = 60°)

Fig. 11 Loading force, F – turning type processes

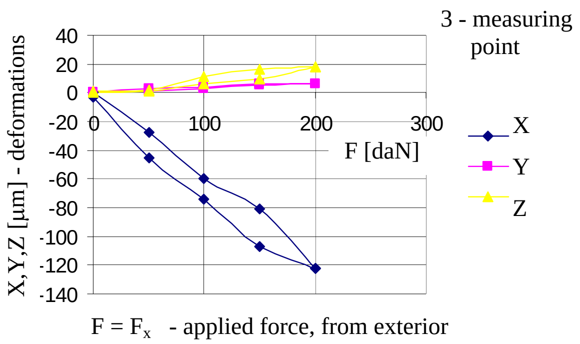

F_x - loading force, from exterior

Fig. 12 Loading with F_x force, from exterior - drilling, milling, punching, bending, drawing type processes

Table 1

Experimental results – for turning type process

F_x [daN]		Deformation [μm] X	Y	Z
0	l	0	0	0
	ul	*0*	*0*	*0*
50	l	0	-21	117
	ul	*-4*	*-13*	*210*
100	l	-7	-45	232
	ul	*-10*	*-40*	*275*
150	l	-13	-68	343
	ul	*-14*	*-80*	*410*
200	l	-16	-96	479
	ul	*-16*	*-96*	*479*

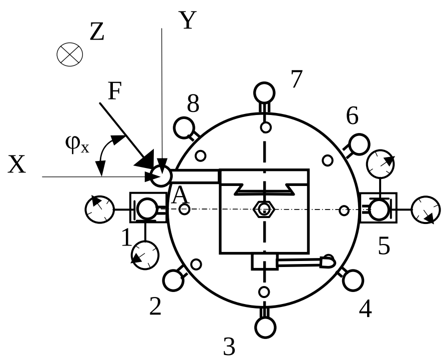

A: loading point

1: measuring point

l: loading
ul: unloading

$\varphi_x = 0°$; ($\varphi_y = 90°$)
$\varphi_z = 90° \Rightarrow F_x$

F_{yz} [daN] ($\varphi_z = 60°$)		Deformation [μm] X	Y	Z
0	l	0	0	0
	ul	*1*	*1*	*0*
50	l	-11	10	-39
	ul	*-13*	*12*	*-32*
100	l	-20	19	-50
	ul	*-24*	*20*	*-61*
150	l	-23	29	-93
	ul	*-27*	*30*	*-96*
200	l	-33	40	-127
	ul	*-33*	*40*	*-127*

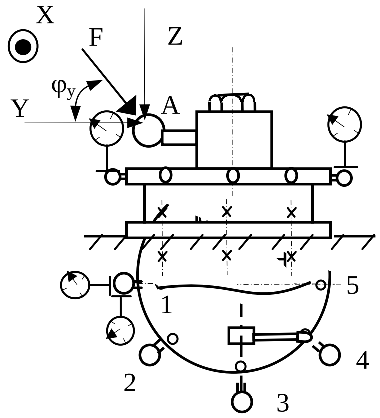

A: loading point

5: measuring point

l: loading
ul: unloading

$\varphi_x = 90°$; $\varphi_y = 30°$
($\varphi_z = 60°$) $\Rightarrow F_{yz}$

Table 2

Experimental results – for drilling, milling, punching, bending, drawing type process

F [daN]		Deformation [μm] X	Y	Z
0	l	0	0	0
	ul	*-3*	*0*	*1*
50	l	-28	1	1
	ul	*-45*	*3*	*2*
100	l	-60	3	6
	ul	*-74*	*4*	*11*
150	l	-81	5	10
	ul	*-107*	*6*	*16*
200	l	-122	6	18
	ul	*-122*	*6*	*18*

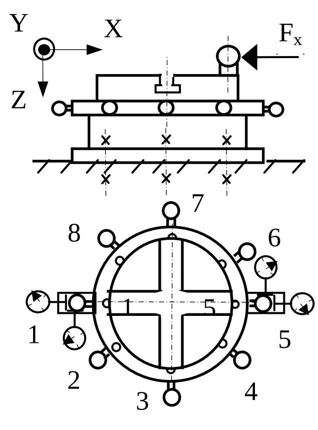

A: loading point

3: measuring point

l: loading
ul: unloading

$F_x \Rightarrow$ applied from the exterior

For the presented examples, the resulting values -- see relation (2) – of strain and rigidity are shown in Table 3.

There were also carried out experiments, in order to check the accuracy of the vibration resonance frequencies, simulated with ANSYS software.

So, the device's dynamic loading was done with a spherical element, weighting *m* [kg], and falling on the device from a height, *h* [mm]. The answering resonance frequency is determined (on the oscilloscope screen) for each experiment.

Table 3

Deformation and rigidity values

F [daN]	Measuring point	Strain, C [mm/daN]			Rigidity, K [daN/mm]		
		$\frac{X_{max}}{F_{max}} \times 10^{-3}$	$\frac{Y_{max}}{F_{max}} \times 10^{-3}$	$\frac{Z_{max}}{F_{max}} \times 10^{-3}$	$\frac{X_{max}}{F_{max}} \times 10^{-3}$	$\frac{Y_{max}}{F_{max}} \times 10^{-3}$	$\frac{Z_{max}}{F_{max}} \times 10^{-3}$
F_x	1	-0.080	-0.480	2.395	-12.500	-2.084	418
F_{yz}	5	-0.165	0.200	-0.635	-6.061	5,000	-1.575
F_x - exterior	3	-0.610	0.030	0.090	-1.640	33,334	11,112

The experiment scheme is shown in Figure 13, while a device's vibration answering curve is presented by Figure 14.

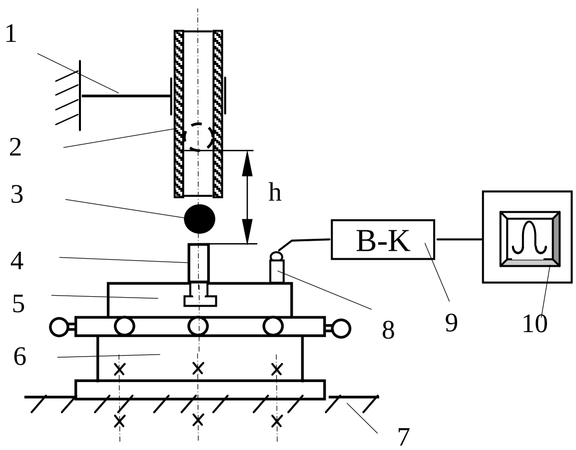

1 – rigid support; 2- guidance cylinder;
3 – spherical element, weight *m*;
4 – additional element; 5 – addition plate;
6 – dynamometer; 7 – rigid mass; 8 – transducer;
9 –Brüel-Kjoer vibrometer; 10 – memory oscilloscope

Fig. 13 Dynamic rigidity experiments scheme

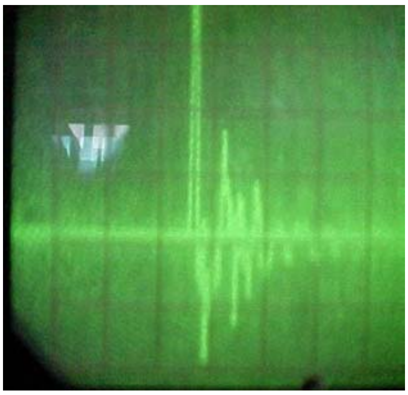

Fig. 14 Vibration answering curve – in dynamic loading

3.4 Calibrating Equation

Calibrating the device, in order to measure manufacturing forces, had to be realized under conditions similar to the ones existing in real situations.

So, as the manufacturing processes conditions vary in a large amount, there have been carried out lots of experiments, each one being characterized by: loading point's position, the direction (Ox, OY, Oz) and values of the loading force, the device's deformations. Thus, under F_ρ (ρ = x, y, z) loading, there is generated the $\varepsilon_{\rho x}$, $\varepsilon_{\rho y}$, $\varepsilon_{\rho z}$ signal to the ''C_x'', ''C_y'' and, respectively, ''C_z'' channels of the electronic bridge.

The scheme of calibrating experiment under F_x loading is shown in Figure 15, and an image, taken while this calibrating experiments, is presented by Figure 16.

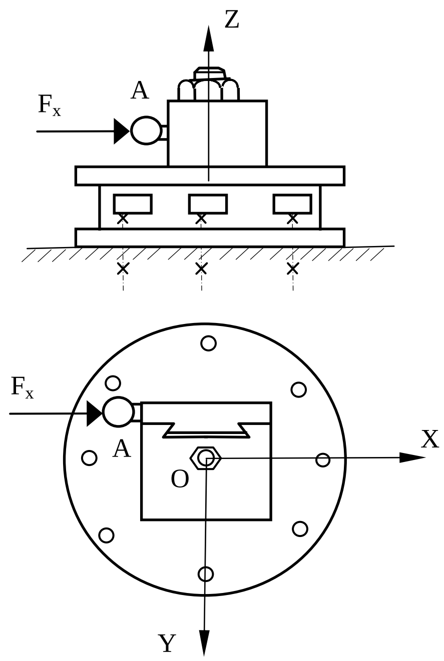

Fig. 15 Scheme of the calibrating process - loading with F_x force

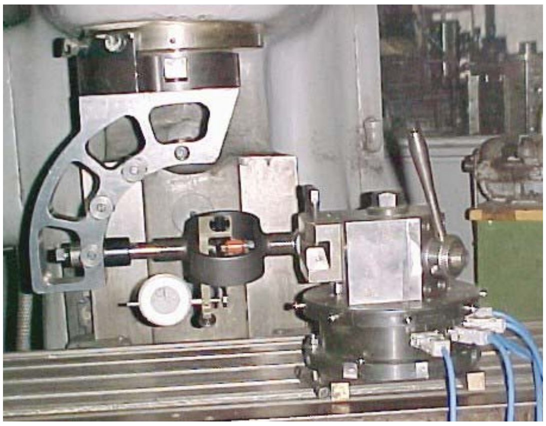

Fig. 16 Calibrating process - loading with F_x force

While a certain force was applied, the corresponding deformations, along each of the reference system's axis, have been measured. There have been obtained linear dependence equations, such as:

$$\varepsilon_{\rho\theta} = a_{\rho\theta} \cdot F_\rho + b_{\rho\theta} \qquad (\rho, \theta = x, y, z) \qquad (3)$$

by adding the effects:

$$\begin{aligned} \varepsilon_x &= \varepsilon_{xx} + \varepsilon_{yx} + \varepsilon_{zx} \\ \varepsilon_x &= \varepsilon_{xx} + \varepsilon_{yx} + \varepsilon_{zx} \\ \varepsilon_x &= \varepsilon_{xx} + \varepsilon_{yx} + \varepsilon_{zx} \end{aligned} \qquad (5)$$

and, consequently, the calibrating equation was:

$$\begin{bmatrix} F_x \\ F_y \\ F_z \end{bmatrix} = \begin{bmatrix} a_{xx} & a_{yx} & a_{zx} \\ a_{xy} & a_{yy} & a_{zy} \\ a_{xz} & a_{yz} & a_{zz} \end{bmatrix}^{-1} \cdot \begin{bmatrix} \varepsilon_x - (b_{xx} + b_{yx} + b_{zx}) \\ \varepsilon_y - (b_{xy} + b_{yy} + b_{zy}) \\ \varepsilon_z - (b_{xz} + b_{yz} + b_{zz}) \end{bmatrix} \qquad (6)$$

An example of the experimentally obtained results is presented in Table 3 (*l* is loading; *ul* is unloading).

Table 3

F [daN]		Deformation [μm] $\varepsilon_{\rho x}$ $(\rho = x, y, z)$		
		F_x	F_y	F_z
0	l	0	-3	0
	ul	*4*	*-4*	*-3*
50	l	219	-9	-12
	ul	*223*	*-9*	*-13*
100	l	431	-15	-38
	ul	*435*	*-16*	*-39*
150	l	641	-21	-54
	ul	*644*	*-23*	*-56*
200	l	835	-29	-78
	ul	*835*	*-29*	*-78*

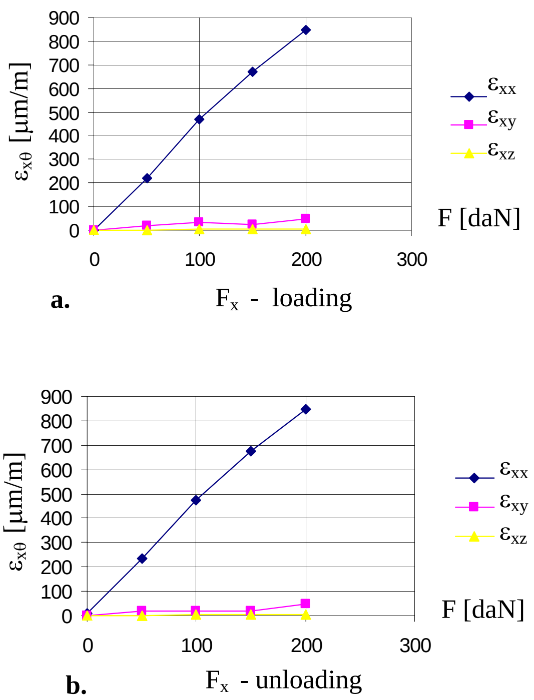

Fig. 17 Calibrating curves – for F_x experiments

The calibrating curves, for the above presented experiments, are shown in Figure 17 (a- is loading and b- is unloading). The regression coefficients have been determined with CurveExpert 1.3 software.

When a Hottinger electronic bridge was used, the calibrating equations obtained are:

- for loading

$$\begin{bmatrix} F_x \\ F_y \\ F_z \end{bmatrix} = \begin{bmatrix} 0{,}2402 & -0{,}0052 & -0{,}0218 \\ -0{,}0092 & 0{,}2443 & -0{,}0181 \\ -0{,}0100 & -0{,}0237 & 0{,}2361 \end{bmatrix} \cdot \begin{bmatrix} \varepsilon_x - 6{,}200 \\ \varepsilon_y - 17{,}600 \\ \varepsilon_z + 4{,}000 \end{bmatrix} \qquad (7)$$

- for unloading

$$\begin{bmatrix} F_x \\ F_y \\ F_z \end{bmatrix} = \begin{bmatrix} 0{,}2412 & -0{,}0052 & -0{,}0214 \\ -0{,}0089 & 0{,}2399 & -0{,}0177 \\ -0{,}0097 & -0{,}0231 & 0{,}2365 \end{bmatrix} \cdot \begin{bmatrix} \varepsilon_x - 14{,}200 \\ \varepsilon_y - 21{,}800 \\ \varepsilon_z - 2{,}200 \end{bmatrix} \qquad (8)$$

3.5 Exploitation of the Designed Device

The device for measuring manufacturing forces, was tested into several technological systems – in both cutting, and metal forming manufacturing processes.

An image taken, while turning, is presented in Figure 18.

Fig. 18 The device used in exterior cylindrical turning of a sample

Table 4

Turning process	Machining parameters			
	t [mm]	s [mm/rot]	v [m/min]	n [rot/min]
TP 1	0.2	0.3	0.4	1
TP 2	0.1	0.14	0.2	0.2
TP 3	150	110	75	75
TP 4	800	600	400	400
	t – cutting depth; s – cutting feed;		v – cutting speed; n – main spindle rotational speed	

There were considered cylindrical (55 mm, diameter) samples, made of OLC 45 and they were submitted to exterior cylindrical turning type process.

The values of cutting process parameters have also been established and presented in Table 4.

In order to measure the turning forces, there has been used a computer aided data acquisition system, LabVIEW, that enabled a sampling rate of 1,000 measures/second, for 5 second, thus, resulting in 5,000 successively measured values, at an interval of 1milisecond.

A detail of the obtained curves is pointed out by Figure 19.

With a specific LabVIEW program – whose schematic structure is presented in Figure 20, there have been calculated the medium values, in volts, for each of the force's components. Taking into account the electronic bridge characteristics and the calibrating equation, there have been obtained the values, in daN, of the manufacturing force.

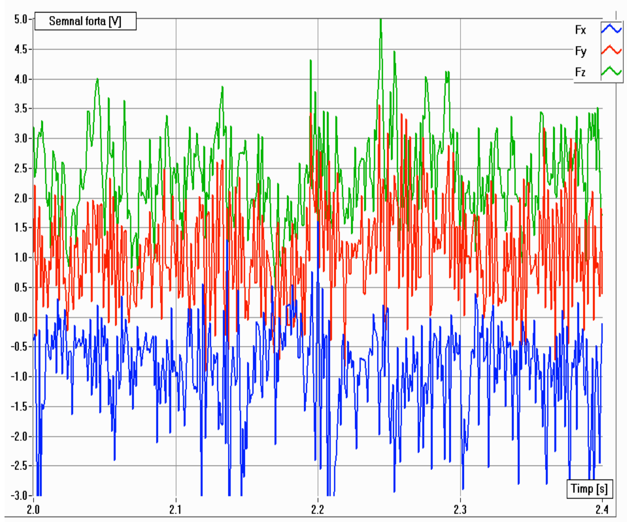

Fig. 19 The curves corresponding to the turning force's components

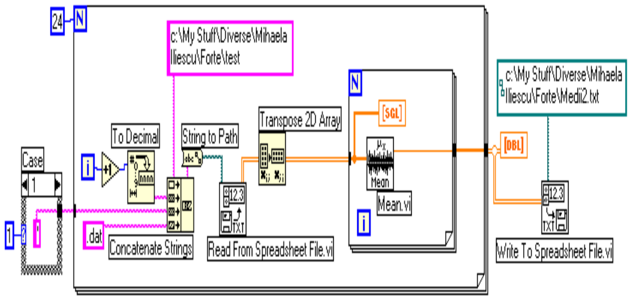

Fig. 20 LabVIEW program for obtaining medium values of measured values

For example, if the values of the cutting parameters were: cutting speed, v = 110 m/min; cutting speed, s = 0.14 mm/rot; cutting depth t = 0.3 mm then, the values of the turning force's components were determined to be: F_x = 7.43 daN, F_y = 6.73 daN, F_z = 4.97 daN, meaning, the global force resulted in F = 11.2 daN.

If, for the considered turning process, the manufacturing force should have been calculated with the relations presented by the specific literature [5] the value for the F_z component of the cutting force results in 12.16 daN. One can notice good concordance between experimentally and theoretically determined values.

The device has, also, been tested into a metal forming process, meaning punching of the part whose drawing is shown in Figure 21.

An image, taken while the tests were on, is presented in Figure 22.

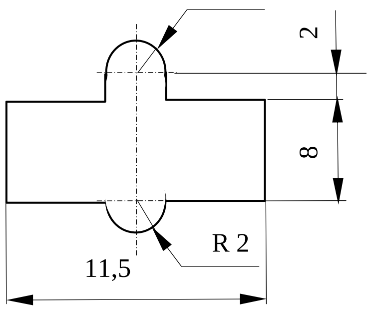

Fig. 21 Drawing of the punched part

Fig. 22 The device used in punching of a sample

The device managed to offer good results, in this kind of manufacturing processes, too. So, if the punching force would have been calculated (knowing the material's thickness, 0.4 mm, and shearing stress value, 30daN/mm^2), the obtained value would have resulted in 713.4 daN.

When using the device for measuring processes' force, based on its calibrating equation and the force variation curve (registered on the oscilloscope screen, the device was connected to – as seen in Figure 23), the obtained value was 710.2 daN.

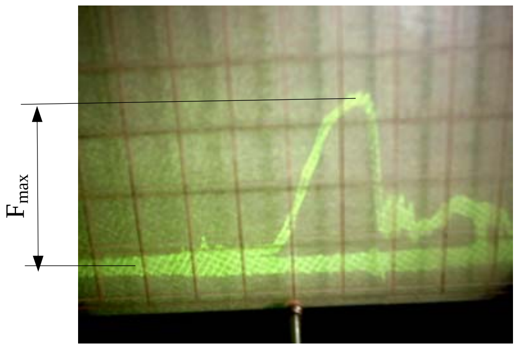

Fig. 23 Punching force variation curve

4 Conclusion

The designed and manufactured device for manufacturing forces' measuring, is characterized by: high rigidity; significant decoupling of the signals corresponding to various loading directions; low weight; easy to use.

All of the above mentioned aspects were theoretically and experimentally determined.

There have been designed and realized all the experimental stands needed, there have been carried out lots of experiments, there have been used modern and complex software and, finally, the experimental results were in concordance with the theoretical ones.

Some important aspects, of the device, should be stated as follows: innovative form of the elastic element; good deformation characteristic and high values for the static rigidity; reliable calibrating equations; possibility to use it in, both, cutting and metal forming manufacturing processes; opportunity for its exploitation into an automated adaptive command system of the manufacturing process.

References:

[1] Cioca L. I., Breaz R. E., Racz G. S., *Multi-Criteria Decision Making Techniques used in Manufacturing Processes Reengineering based upon Modelling and Simulation*, WSEAS Transactions on Systems, Issue 12, vol. 5, pag. 2813, December 2006, ISSN 1109-2777

[2] Constantinescu I. N., ş.a., *Măsurarea mărimilor mecanice cu ajutorul tensometriei*, Editura Tehnică, Bucureşti, 1989.

[3] Iliescu M., Turdeanu E., "*Static Rigidity and Specific Deformation of a Designed Dynamometer for XOZ Plan Turning Type Loading*", The 7th International Conference – TQSD 06, pag. 197-202, ISBN 973-720-035-7, Bucharest, 2006.

[4] Medel J De Jessus, Hernandez G., Guevare P., *Real Time Flexible Manufacturing System, Proceedings of 10th* WSEAS on Automatic Control, Modelling & Simulation pag. 286, ISSN 1790-5117, Istanbul, 2008.

[5] Roy R., Chatelain J-F. at al., *Programming of a Machining Procedure for Adaptive Spiral Cutting Trajectories, Proceedings of 10th* WSEAS on Automatic Control, Modelling & Simulation pag. 127, ISSN 1790-5117, Istanbul, 2008

[6] Turdeanu, E., *Contribuții le dezvoltarea captoarelor de măsurare a forțelor de prelucrare*, Teză de doctorat, Bucureşti, 2004.